Journal of Biomedical Optics

SPIEDigitalLibrary.org/jbo

Study of plasma-induced peripheral blood mononuclear cells survival using Fourier transform infrared microspectroscopy

Ranjit K. Sahu
Ahmad Salman
Shaul Mordechai
Esther Manor

SPIE

Study of plasma-induced peripheral blood mononuclear cells survival using Fourier transform infrared microspectroscopy

Ranjit K. Sahu,[a,b] Ahmad Salman,[c] Shaul Mordechai,[a] and Esther Manor[d]
[a]Ben Gurion University, Department of Physics and the Cancer Research Institute, Beer Sheva 84105, Israel
[b]The Feinstein Institute for Medical Research, Center for Autoimmune and Musculoskeletal Diseases, 350 Community Drive, Manhasset, New York 11030
[c]SCE-Shamoon College of Engineering, Department of Physics, Beer Sheva 84100, Israel
[d]Soroka University Medical Center, Department of Cytogenetics, Beer Sheva 84105, Israel

Abstract. Components present in the acellular fraction of blood influence the blood cell survival and function and the response to biotic and abiotic factors. Human plasma and sera have been used as therapeutic agents and are known to increase cell survival. White blood cells in normal blood are exposed to plasma components *in vivo*, but the effect of such plasma components *in vitro* on adherent peripheral blood mononuclear cells (PBMCs) that includes monocytes has not been fully investigated. We cultured human PBMCs with autologous plasma and observed structural variation due to plasma addition in PBMCs along with increased cell survival. Light microscopy of the cells showed increased granularity in plasma-treated cells. Fourier transform infrared (FTIR) spectroscopy was used to elucidate the possible mechanism by studying the changes in the biochemical composition of the cells that explained the observations. FTIR spectroscopy of plasma-treated cells show altered spectral pattern in the mid-IR region, indicating increased phospholipid levels. Heat-stable components in the plasma possibly increase the differentiation of PBMCs, as evident by increased phospholipid metabolism. The data suggest that plasma-stimulated membrane biogenesis may contribute to PBMC survival by inducing them to differentiate into antigen presenting cells (APCs) like macrophages and dendritic cells. [DOI: 10.1117/1.JBO.18.11.115004]

Keywords: peripheral blood mononuclear phagocytes; phospholipid metabolism; Fourier transform infrared microspectroscopy.

Paper 130625R received Aug. 29, 2013; revised manuscript received Oct. 16, 2013; accepted for publication Oct. 25, 2013; published online Nov. 18, 2013.

1 Introduction

Peripheral blood mononuclear cells (PBMCs) consist of a diverse group of white blood cells (WBCs) responsible for both adaptive and innate immune responses. With an increasing awareness of the role of these cells and the challenge of understanding the mechanisms that lead to their differentiation into different subtypes with specific functions, *in vitro* studies have become essential. Components present in the complex mixtures of blood plasma/serum play a regulatory role in development and differentiation of the immune cells. Utility of autologous serum during ophthalomological surgeries has been studied with a view to understand its implication for rapid recovery, since the autologous serum has many useful metabolites that help in tissue repair while being devoid of artificial preservatives.[1–3] Autologous-conditioned serum has been evaluated for treating osteoarthritis (OA) by studying the different levels of cytokines present and their net effect on the OA cartilage explants.[4] Treatment of monocytes with autologous serum indicated a change in surface expression of toll-like receptors and human leukocyte antigen, though they were not found to be related to blood serum factors.[5] Similarly, metabolites in plasma affect monocytes function.[6] Several factors can affect the biochemical and metabolic patterns of cultured cells including the nutrient sources, growth conditions, and cell source. Culturing of PBMCs is routinely undertaken to understand cellular mechanisms responsible for immunity. Conventionally, human PBMCs are cultured for *in vitro* studies using heat-inactivated fetal calf serum (FCS) as a source of essential nutrients (amino acids). Utilization of autologous human plasma (AHP), which can be obtained (during routine separation of PBMCs) from blood, has not been evaluated as an alternative to FCS. Similarly, replacement of blood volume by plasma volume expanders is being studied, so that loss of plasma can be compensated during accidents and blood loss. However, plasma components can affect the PBMCs and hence maybe indispensible. With advent of newer technologies, there is a trend of preserving blood cells and reintroducing them in the future with a presumption that the cells would be more compatible originating from the same person. Thus, understanding monocytes-related complications are important in transfusion medicine[7,8] while designing suitable plasma substitutes. Infrared spectroscopy has been utilized to monitor cellular metabolism and to differentiate them using spectral characteristics.[9–11] Serum supplementation plays an important role in cell viability by detoxification.[12] Thus, we undertook an Fourier transform infrared (FTIR) spectroscopy-based

Address all correspondence to: Ranjit K. Sahu, The Feinstein Institute for Medical Research, Center for Autoimmune and Musculoskeletal Diseases, 350 Community Drive, Manhasset, New York 11030. Tel: +001-3473317073; Fax: 516-562-2593; E-mail: ranjit@bgu.ac.il or Shaul Mordechai, Ben Gurion University, Department of Physics and the Cancer Research Institute, Beer Sheva 84105, Israel. Tel: 972-8-6461749; Fax: 972-8-6472924; E-mail: shaulm@bgu.ac.il

0091-3286/2013/$25.00 © 2013 SPIE

investigation on the effect of replacement of FCS with AHP or nonautologous-pooled human plasma (NAHP) during the culture of human PBMCs.

Using infrared spectroscopy, we attempted to elucidate the biochemical changes occurring in PBMCs due to the addition of AHP/NAHP. These biochemical changes could explain observations made on monocytes,[4–6] since FTIR microspectroscopy (FTIR-MSP) has been widely used to study biochemical changes during cell growth and metabolism.[13–15] FTIR-MSP has an ability to provide simultaneous quantification of different metabolites and to identify them through unique spectral fingerprints, overcoming the requirement of separate analytical techniques for each biochemical component in low-abundant samples. PBMCs of healthy volunteers cultured in media supplemented with AHP/NAHP resulted in altered morphological features and increased cell viability. Microscopic examination indicated increased granularity in cells exposed to AHP, which implied increased differentiation of the adherent PBMCs. Biochemical changes analyzed using FTIR spectroscopy showed increased levels of phospholipids in cells exposed to AHP/NAHP. The present study indicates that replacement of FCS by AHP in the culture media affects the cell dynamics and metabolism mainly through the activation of phospholipid metabolism.

2 Materials and Methods

2.1 *Isolation, Culture, and Microscopic Evaluation of PBMCs*

1. Peripheral blood was collected from healthy volunteers with their consent, and adherent cells were separated and cultured in RPMI-1640 medium (Roswell Park Memorial Institute), supplemented with antibiotics and glutamine (Biologic Industries, Beit-Haemek, Israel). Samples were supplemented with NAHP, AHP, or heat-inactivated FCS.[16] All samples were incubated at 37°C in a 5% CO_2 atmosphere for a period of 12 to 13 days. After that, AHP- and NAHP-treated cells were observed under the dark field for signs of luminescence. The cells were harvested mechanically using a rubber policeman, washed in phosphate-buffered saline (PBS), and re-suspended in normal saline. One microliter of the cell suspension was spotted on a ZnSe window and allowed to air dry in a laminar air flow chamber for several hours before FTIR microscopy.

2. Cells were cultured over sterile glass cover slips as above. The media was removed, and the cover slips were rinsed with PBS. They were then fixed in ice cold methanol for a minute and again rinsed in PBS to remove the methanol. Light microscopy was also done on live cells in the wells to monitor changes in morphology.

3. Live cells were counted after staining with trypan blue. The quantity of live cells was normalized to the number of live cells in heat-inactivated FCS-supplemented media to compensate variability due to donors and experiments. Each reading was the average of duplicates or triplicates depending on the amount of PBMCs obtained.

4. AHP was prepared as described previously[17] from the peripheral blood of the same volunteer and added in the required amount as described previously. NAHP was prepared in a similar manner from a pool of four to eight donors.

2.2 *FTIR Microspectroscopy*

Measurements of cells mounted on ZnSe slides were performed using the FTIR microscope IRscope II with a liquid nitrogen cooled mercury-cadmium-telluride detector, coupled to the FTIR spectrometer (Bruker Equinox model 55 OPUS software), as reported previously.[13] To achieve high signal-to-noise ratio, 128 or 256 co-added scans were collected in each measurement in the wavenumber region 600 to 4000 cm^{-1}. The measurement site was circular with a diameter of 100 μm. This area was found earlier to contain about 100 cells for analysis by FTIR-MSP. For each sample, at least five measurements were made at randomly selected sites on a monolayer of cells. The spectra were cut into two regions: 2750 to 3050 cm^{-1} for the higher wavenumber region and 900 to 1800 cm^{-1} for the mid-IR region. The obtained spectra were baseline corrected separately in each wavenumber region using the rubber band correction method with 64 consecutive points in the OPUS software. The spectra were normalized to the CH_2 antisymmetric (asym) band in the higher region or to the amide I absorbance band for the lower wavenumber region. The normalized spectra were averaged, and the deduced spectra were used for subsequent calculations and analyses. Normalization to amide II or use of vector normalization for the entire spectra did not significantly alter the results. Since the ratios are sensitive to baseline correction, the same procedure was adopted systematically for all samples and all spectral analysis. For cluster analysis, principal component analysis (PCA) and linear discriminant analysis (LDA) calculations spectra were bisected into two ranges: the low region 600 to 1800 cm^{-1} and the high region 2750 to 3050 cm^{-1}. The spectra were baseline corrected in each region separately using the concave rubber band correction method, normalized using vector normalization methods, and then were offset using the OPUS 7 software.

2.3 *Statistical Analysis*

Our main goal in this study is to understand the effects of FCS, AHP, and NAHP on biochemical changes of PBMCs. It was difficult to differentiate between the effects of AHP and NAHP with a high-success rate using FTIR spectra and the biological biomarkers and both showed similar functional effects on the PBMCs. In order to understand the relative differences between the treatments and to obtain good classification between the investigated samples, we used advanced computational methods—supervised and unsupervised pattern recognition techniques—PCA, LDA, and clustering as discussed below.

2.3.1 *Principal component analysis*

PCA is a mathematical algorithm that reduces the dimension of the problem that is being dealt with.[18,19] In other words, instead of using many variables (hundreds), the variability in the data is described using only few PCs.[19–21]

Using PCA algorithm, we obtain a new multidimensional space based on the variability of the data. The new directions

(axes) are referred to as PC1, PC2, and so on. The PC1 axis (first principle component) contains the highest variance. The second principal component (PC2) accounts for most of the residual variance and is perpendicular to the first one. The subsequent principal components obey the same rules.

PCA is widely used in pattern recognition[20–22] and identification problems with the assumption that the most separable directions are those with the highest variance.

2.3.2 *Linear discriminant analysis*

Following PCA, LDA was performed.[23,24] Using LDA algorithm, a linear combination of the variables is generated which maximize the variance between the categories and minimize the variance in the interclass. LDA was used to discriminate between different categories NAHP, AHP, and FCS. A training set (part of the data measurements) is used to construct the linear combination and the others are used for test.

Training and test sets were selected randomly from the database. Examination of the results was performed using the variant "leave-one-out" (LOO),[25,26] (usually applied with small amount of data) when $k = N$, the number of data points.[27,28]

2.3.3 *Cluster analysis*

Cluster analysis[29,30] is an unsupervised technique that uses the distance between spectra in order to cluster them according to their nearness in the row space. It shows the data in a two-dimensional (2-D) plot (name of file versus heterogeneity), referred to as dendrogram.[30,31] Unsupervised cluster analysis was performed on the average spectra of samples at different regions 900 to 1800 cm^{-1} and 2750 to 3050 cm^{-1}.

3 Results

Supplementation with AHP led to an increased survival of adherent cells derived from peripheral blood compared with growing the cells in only FCS-supplemented media. Study of the effect of the variation of AHP on the number of viable cells in culture after 14 days showed that even at the lowest studied levels (2%), AHP promoted the viability of the cells by two to three folds, and this trend was sustained with increasing the amount of AHP [Fig. 1(a)].

Representative images of adherent cells grown in RPMI media supplemented with AHP or FCS (10%), as seen under an optical microscope, are shown in Fig. 1(b), i and ii, respectively. The cells treated with AHP [Fig. 1(b), ii] were larger, more granular, and also oval to circular compared with the FCS-treated cells [Fig. 1(b), 1(i)], which were elongated. The cells treated with AHP had a tendency of increased granularity of the cells with a large number of vacuoles in the cytoplasm [Figs. 1(b) and 1(d)]. The cells treated with autologous plasma were luminescent in a dark field when viewed under the microscope, and the luminescence increased with increasing levels of AHP, though a further quantification was not carried out. The control FCS-treated cells did not have a significant amount of luminescence and were similar to the dark background [Fig. 1(c)]. The increasing cell size and granularity may partly account for the increased luminescence at higher concentration of AHP along with increasing levels of phosphorescent

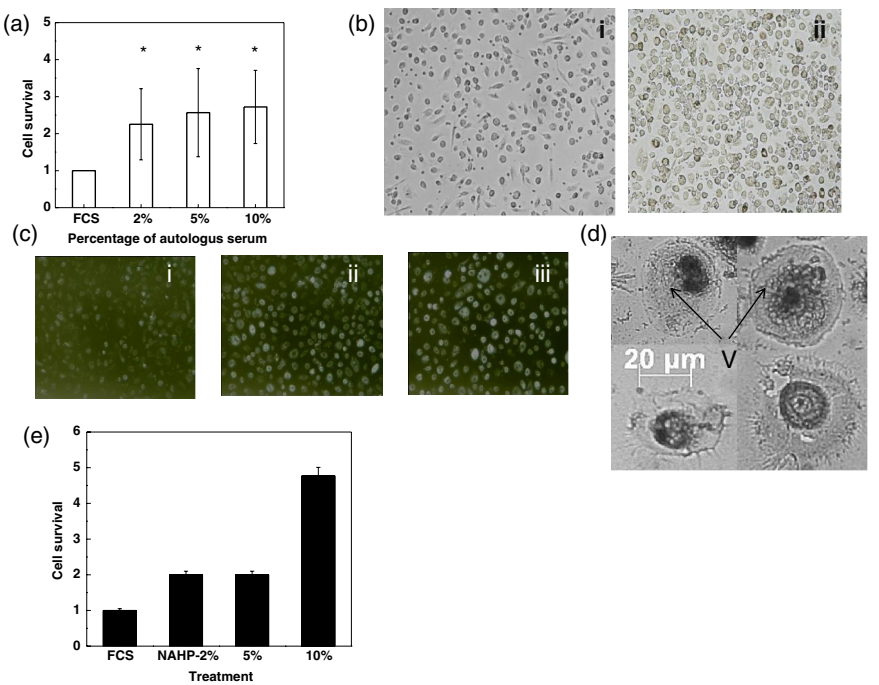

Fig. 1 Peripheral blood mononuclear cells (PBMCs) cultures in media with heat-inactivated fetal calf serum (FCS) or autologous human plasma (AHP). (a) Relative amount of surviving cells compared with heat-inactivated FCS (data are averages of four independent experiments with each sample duplicated) Asterisks indicate significant difference at $p < 0.05$ between control and treatments. (b) As observed under a light microscope. (i) Cultured with heat-inactivated FCS (10%) and (ii) AHP (10%). 5×10^5 cells were plated for 10 to 12 days after purification. Images shown are under magnification of ×10 and are representative of three independent experiments. (c) As observed under dark field after culturing with AHP. (i) 2%, (ii) 5%, and (iii) 10%. 5×10^6 cells were plated for 10 to 12 days after purification. Images shown are under magnification of ×10 and are representative of three independent experiments. The control cells had no luminescence in the dark field compared with the background luminescence. (d) Higher magnification of cultured cells shows increased vacuolation (V) in cells treated with AHP (top) compared with heat-inactivated FCS (bottom). (e) Survival of PBMCs in presence of nonautologous-pooled human plasma (NAHP).

compounds. An increase in cell survival was also observed when NAHP was used instead of AHP [Fig. 1(e)]. The pooled NAHP may provide more heterogeneous stimuli compared with AHP, which may reflect the partial increase seen in case of NAHP compared with AHP.

Further studies were undertaken to understand the mechanism that could possibly explain the observed improvement in survival rates. FTIR spectral analysis of the samples was carried out, since FTIR spectroscopy has the potential to analyze the different biological macromolecules in terms of their functional groups. Moreover, normalization of the components can be achieved to overcome problems occurring due to cell number and morphology without having to resort to any analytical biochemical methods that may require cell processing and loss of biochemical information. This methodology is also useful to obtain extensive biochemical information from small quantities of cells available after purification and culturing. Figure 2(a) shows the FTIR spectra in the higher wavenumber region (2750 to 3050 cm^{-1}). It was noted that the treatment with AHP resulted in the appearance or prominence of a band around ~3010 cm^{-1} (corresponding to the olefinic groups[32]) with a decrease in the intensity associated with the CH_3 asym stretching vibrations. Simultaneously, an increase in the intensity at 2852 cm^{-1} was seen which originates due to the CH_2 sym stretching, which corresponds to membrane lipids. This indicated an increased presence of membrane bound lipids or presence of organelles in the cells treated with AHP compared with the FCS samples. Further examination of the spectra in the lower region between 900 and 1800 cm^{-1} showed a sharp band near 1740 cm^{-1} [Fig. 2(b)], which corresponds to fatty acid esters.[14,15] The second-derivative spectra [Fig. 2(d)] also indicated that there was an increase in lipid components in cells supplemented with AHP as compared with FCS. Signature absorbance bands were seen at 1743, 1468, 1240, 1170, and 970 cm^{-1}, which corresponds to wavenumbers where phospholipids and esters are known to absorb.[32] An increase in intensity at these wavenumbers in the baseline-corrected spectra and increased minima in the corresponding second-derivative spectra [Figs. 2(c)–2(e)] confirmed that these bands arise from phospholipids, which are principal components of the membranes of cells and tissues.

An interesting extension of the above observations is the effect of the NAHP on the above properties of the cells. This aspect was studied with a view that it may be used to substitute AHP when the latter is not available in abundance. Examination of the infrared absorbance spectra revealed that the spectral variation due to the addition of NAHP was similar to that of AHP [Figs. 3(a) and 3(b)]. The second-derivative spectra again showed minima at the wavenumbers similar to those seen earlier in the spectra of AHP-treated cells [Figs. 3(c)–3(e)]. Importantly, the cell survival in presence of NAHP was also higher than of FCS [Fig. 1(e)]. Thus, our results indicate that

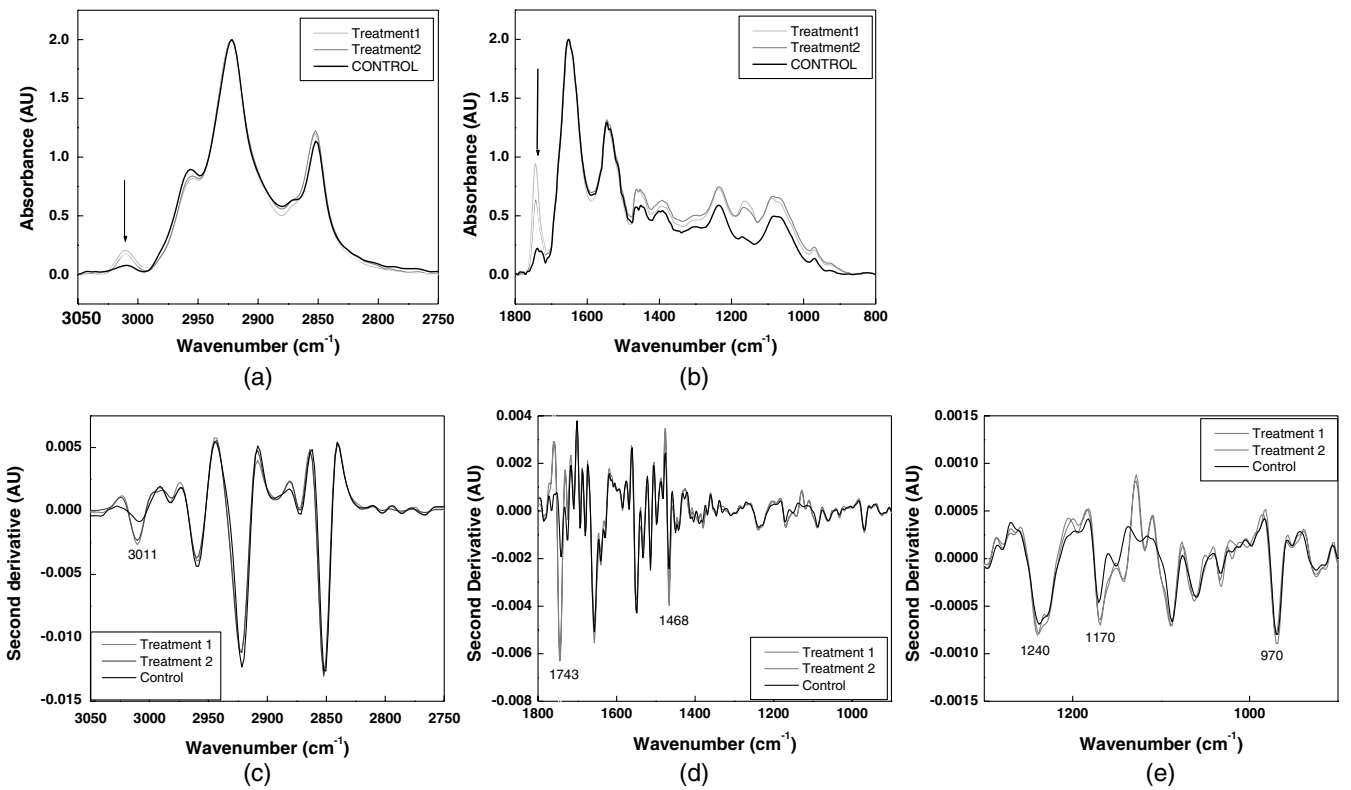

Fig. 2 Effect of AHP on PBMCs FTIR spectra (a) in the region 2750 to 3050 cm^{-1} (arrow indicates band at ~3010 cm^{-1} corresponding to olefinic groups) and (b) in the region 800 to 1800 cm^{-1} (arrow indicates band at ~1740 cm^{-1} corresponding to esters). (c) Second-derivative spectra in the region 2750 to 3050 cm^{-1} showing increased levels of lipids components with unsaturated vibrations and membrane lipids. The minima are labeled and correspond to maxima in the original spectra. (d) Second-derivative spectra in the region 1800 to 1000 cm^{-1} showing increased intensity at 1468 and 1743 cm^{-1} corresponding to lipids. (e) Second-derivative spectra in the region 800 to 1000 cm^{-1} showing increased intensity at 1240, 1170, and 970 cm^{-1} corresponding to phospholipids. The plasma is from two different preparations, represented by treatments 1 and 2. Control refers to heat-inactivated FCS-treated cells. Black lines represent cells cultured with FCS, and gray/light gray lines represent cells treated with autologous plasma in all panels.

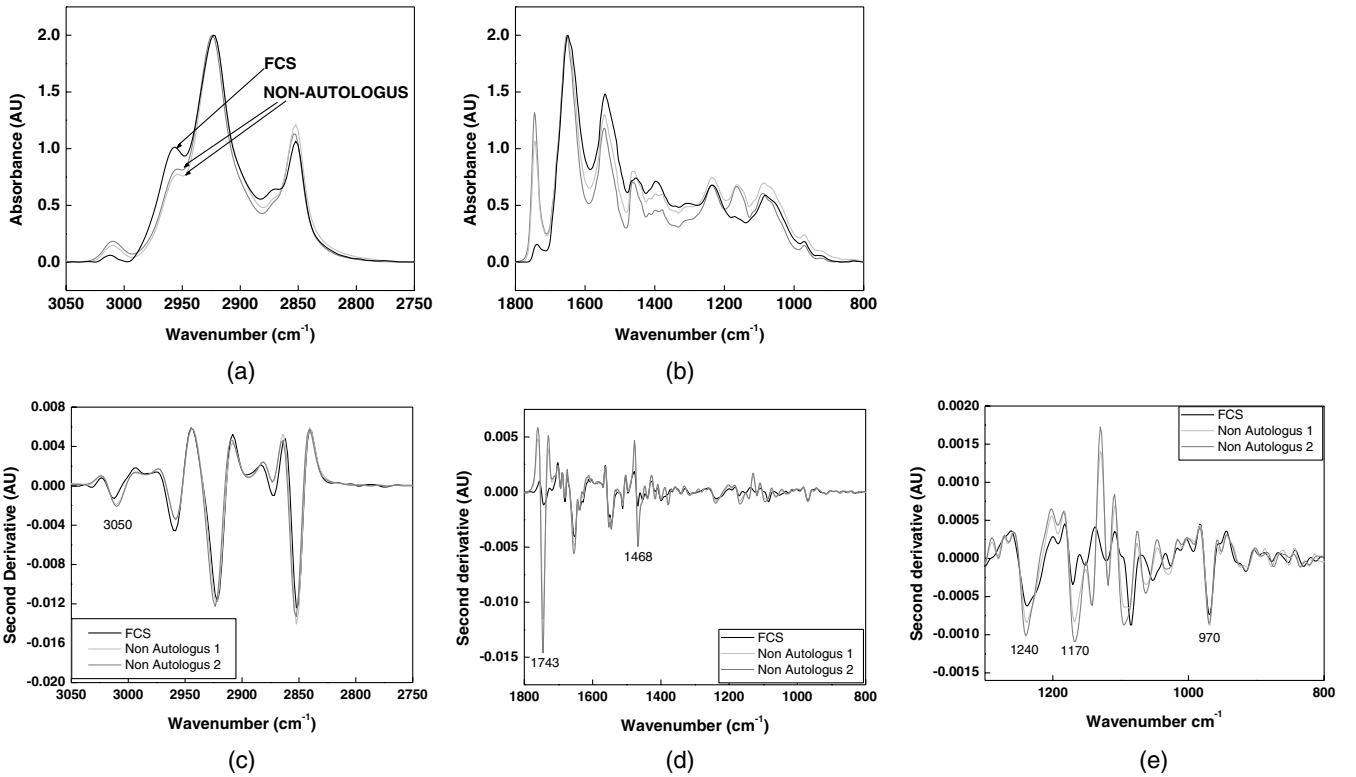

Fig. 3 Effect of NAHP on PBMCs FTIR spectra (a) in the region 2750 to 3050 cm^{-1} (please note the band at ~3010 cm^{-1} corresponding to olefinic groups) and (b) in the region 800 to 1800 cm^{-1} (please note the band at ~1740 cm^{-1} corresponding to esters). (c) Second-derivative spectra in the region 2750 to 3050 cm^{-1} showing increased levels of lipids components with unsaturated vibrations and membrane lipids. (d) Second-derivative spectra in the region 1800 to 1000 cm^{-1} showing increased intensity at 1468 and 1743 cm^{-1} corresponding to lipids. (e) Second-derivative spectra in the region 800 to 1000 cm^{-1} showing increased intensity at 1240, 1170, and 970 cm^{-1} corresponding to phospholipids. The plasma is from two different pools of donors represented by nonautologous 1 and nonautologous 2. Black lines represent cells cultured with heat-inactivated FCS, and gray/light gray lines represent cells treated with nonautologous plasma in all panels.

the factors present in the plasma not only promote cell survival, but also alter cell structure and biochemical composition of PBMCs. This may explain the observations in previous reports,[5,6] where increased functionality of the immune system was obtained by the addition of serum or plasma components.

Variation in the proportion of cells in different stages of cell cycle may be manifested as a change in the absorbance of phosphates (varying due to the absorbance from nucleic acids[13–15]) and increased membrane synthesis in dividing cells. We next analyzed the spectra to further confirm that phosphate absorbance was related to cell differentiation rather than cell proliferation that lead to the observed increase in cell survival. The relative number of cells in the G1 phase in different treatments was evaluated from the intensities at 1087 and 1400 cm^{-1} and the slope between 1051 and 1066 cm^{-1}.[33] The values obtained from different treatments were comparable, though a tendency existed for cells treated with AHP and NAHP to have a lower proportion of dividing cells (Fig. 4) or conversely more of differentiated cells as shown in Fig. 1(d). Further, an increase in the RNA/DNA ratio, calculated from the intensity ratio (1121/1020 cm^{-1}), was observed in cells cultured with AHP. This indicates increased transcription, which may be due to activation of the cells in response to the stimuli from AHP [Fig. 4(d)]. A similar analysis using ratio of intensities for the levels of lipids indicates increased lipids in cells treated with AHP or NAHP, confirming the increasing tendency of RNA synthesis in these cells compared with control [Fig. 4(e)]. Thus, the process of differentiation rather than proliferation seems to be the mechanism by which survival was increased in cells exposed to AHP/NAHP.

Both AHP and NAHP increased cell survival, and gross alterations were observed in the spectral characteristics, as seen in Figs. 2 and 3. Based on the spectroscopic changes in the infrared absorption spectra due to the AHP and NAHP treatments, we tried to differentiate among the three categories FCS, AHP, and NAHP. It was difficult to differentiate among them with appropriate success using simple methods like intensities differences and biological biomarkers. Thus, we tried advanced mathematical and statistical methods. First, we tried unsupervised pattern recognition cluster analysis method with Ward algorithm to assess if there is a difference in the composition between the different treatments. Using cluster analysis, it was possible to differentiate the NAPH from the other two categories, as shown in Fig. 5. For this analysis, we tried different regions of the spectra. One of these plots which gave good results is presented in Fig. 5. It is observed that the FCS- and AHP-treated cells are clustered closer than the NAHP group. Second, we tried more sophisticated methods, like PCA and LDA, for the classification between the FCS and AHP categories, since the clustering results for these classes are poor.

Prior to the LDA calculations, we performed a PCA calculation which is a standard approach for dimensionality reduction, and is widely used in pattern recognition.[18–20]

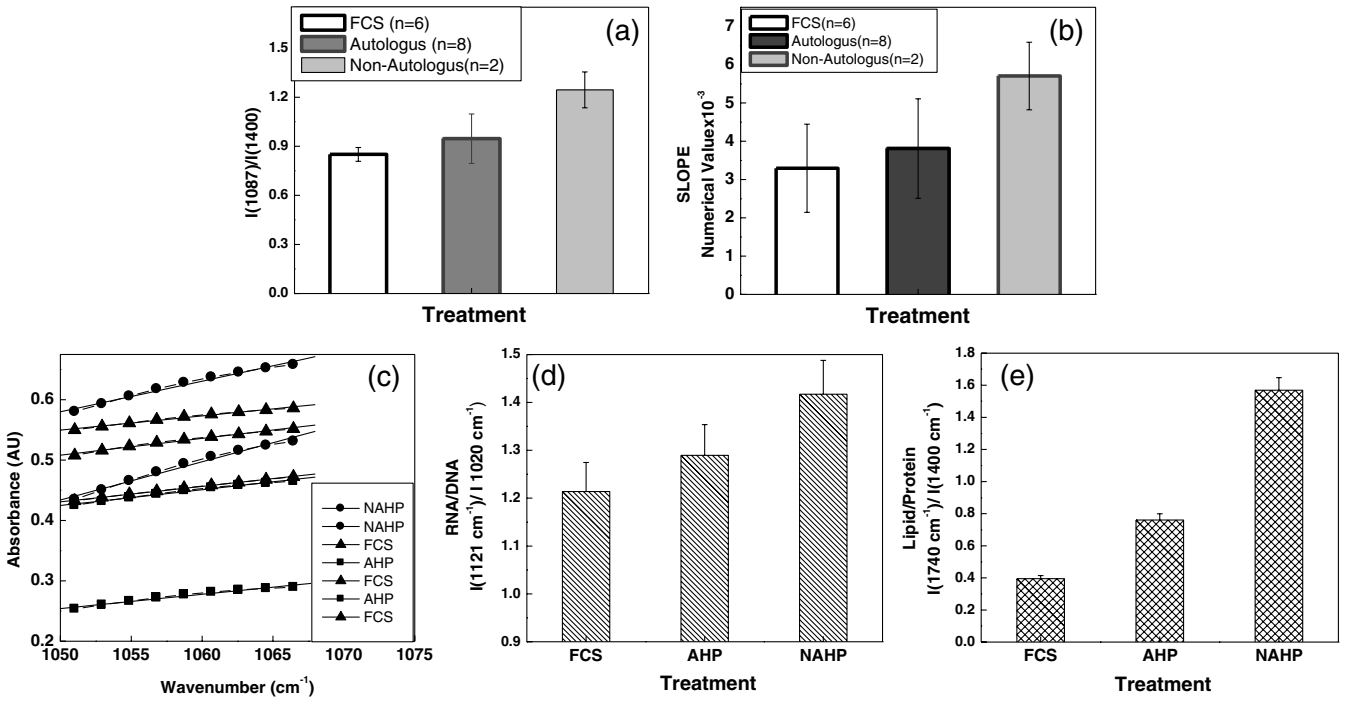

Fig. 4 Effect of AHP and NAHP treatments on cell division of PBMCs determined from (a) ratio of the intensities at 1087 and 1400 cm^{-1} representing phosphates and proteins, respectively, and (b) slopes of the spectra in the wavenumbers region between 1051 and 1066 cm^{-1} representing spectra of samples treated with AHP, NAHP, or FCS. (c) Slopes of the data in the spectral region between 1050 and 1075 cm^{-1} for the indicated samples representing similar proliferation levels. (d) RNA/DNA ratio calculated from the intensities at 1121 and 1020 cm^{-1}. (e) Normalized lipid levels calculated from the intensities at 1740 and 1400 cm^{-1}.

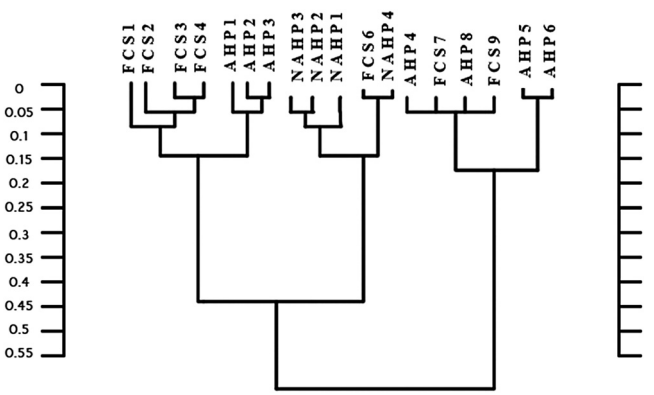

Fig. 5 Dendrogram presentation of the supervised cluster analysis of the AHP, FCS, and NAHP samples. The calculation was performed using the absorbance intensities of phospholipids at 2957, 2924, 2871, 2853, 1732, 1467, 1456, 1402, 1380, 1233, 1171, 1159, 1082, and 1060 cm^{-1} derived from the averaged spectra.

The PCA was undertaken to further establish that the FCS and AHP cells were identical in their chemical composition compared with the NAHP-treated cells. After the PCA calculation, we tested different 2-D plots in order to differentiate among the three categories FCS, AHP, and NAHP. For example, Fig. 6(a) shows the 2-D plots of the data. Each group has its own color. Figure 6(a) clearly shows that it is possible to differentiate completely between NAHP and the other two categories.

LDA calculations were performed using the LOO method on three different regions: region I (1800 to 800 cm^{-1}), region II (3050 to 2750 cm^{-1}), and combined region III (3050 to 2750 and 1800 to 800 cm^{-1}). The differentiation success rates as a function of the first few PCs for the three regions and the variance covered by each PC are listed in Table 1. Also, the identification results of the spectra using seven PCs and region I (1800 to 800 cm^{-1}) are listed in Table 2. It can be seen again that the NAHP samples could be differentiated completely, while overlap existed between the FCS and the AHP categories.

Our calculations lead to one major conclusion, that the NAHP samples have large differences from the other two groups, while the differences between the FCS and AHP are relatively much smaller [Fig. 6(a)]. Therefore, a two-step separation strategy was applied. In the first step, the NAHP-treated cells were separated by considering the FCS- and AHP-treated cells together as a single group (figure not shown). In the next step, the AHP-treated cells were separated from the FCS-treated cells [Fig. 6(b)]. The data indicate that though both AHP and NAHP induce similar changes, the AHP-induced changes are closer to FCS treatment.

As can be seen from Fig. 6(c), in the first strategy, the NAHP was separated with more than 97% success using the first PC and 100% success rate using four PCs, and in the second strategy, the FCS and AHP were separated with 97.7% success rate using seven PCs [Figs. 6(b) and 6(c)].

4 Discussions

PBMCs consist of a diverse group of WBCs responsible for both adaptive and innate immune responses. With an increasing awareness of the role of these cells and the challenge of understanding the mechanisms that lead to their differentiation into subtypes for specific functions, culturing these cells *in vitro* is becoming a trend. Use of vibrational spectroscopy to understand lipid metabolism using FTIR and Raman spectroscopies

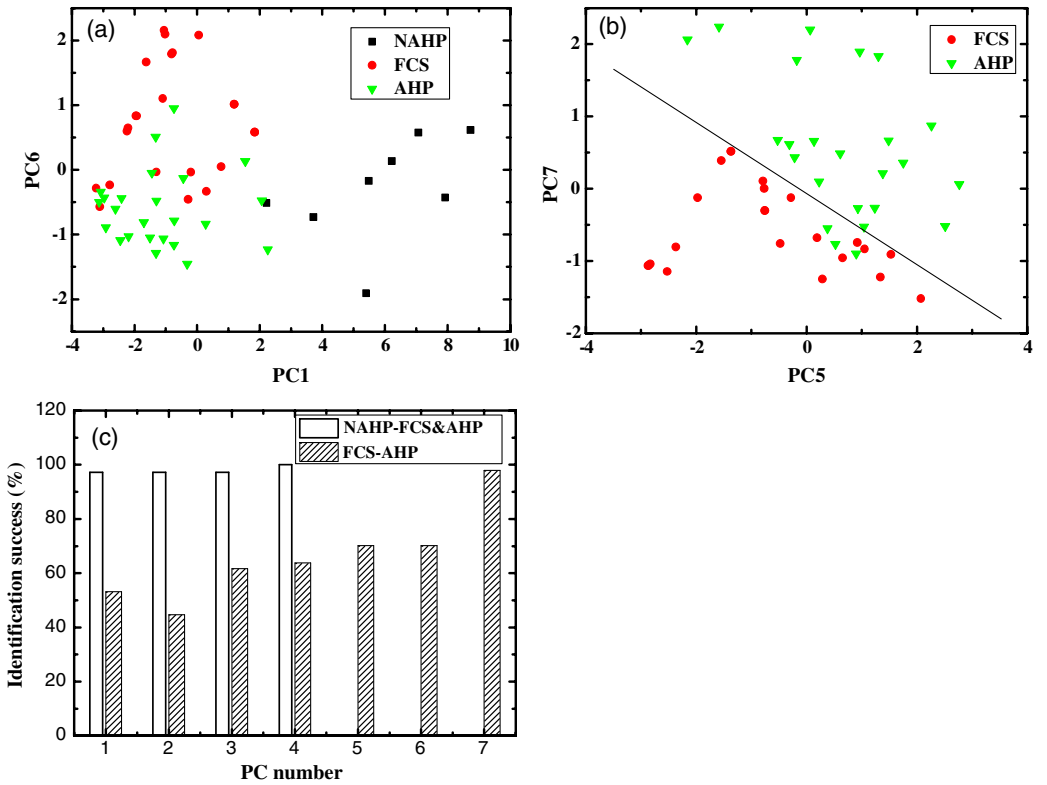

Fig. 6 Separation of the samples using a two-step principal component analysis (PCA): (a) Step 1, two-dimensional (2-D) plots of the AHP, NAHP, and FCS samples based on the PCA calculation in the region 800 to 1800 cm^{-1}. (B) Step 2, 2-D plots of AHP and FCS samples based on the PCA calculation in the same region. (C) Identification success rates in percentage of NAHP versus FCS and AHP and FCS versus AHP based on linear discriminant analysis (LDA) calculations using leave-one-out (LOO) algorithm. The calculations were performed in region I (1800 to 800 cm^{-1}).

Table 1 Differentiation success rates of NAHP, AHP, and FCS samples based on LDA calculations using LOO algorithm in three regions of the spectra and the variance covered by each PC.

PC No.	Variance covered by each PC (%)	Region I (1800 to 800 cm^{-1})	Region II (3050 to 2750 cm^{-1})	Region III (3050 to 2750 and 1800 to 800 cm^{-1})
1	59.95	56.4	43.6	41.4
2	24.98	47.3	67.3	58.6
3	5.99	67.3	67.3	60.3
4	3.65	65.5	67.3	55.2
5	2.27	60	72.7	53.4
6	0.93	78.2	74.5	46.6
7	0.68	96.4	74.5	72.4

Table 2 Successful identification of NAHP, AHP, and FCS samples based on LDA calculations using LOO algorithm and the first nine PCs. The analysis was done in region I (1800 to 800 cm^{-1}).

	NAHP	AHP	FCS
NAHP	8	0	0
AHP	0	22	1
FCS	0	1	23

has been recently reported.[34] Spectroscopic techniques are increasingly being used to study cell metabolism in different systems.[35–37] Of the different groups of WBCs present in the peripheral blood, the monocytes are important as they have a propensity to differentiate into antigen-presenting cells (APCs), like macrophages and dendritic cells (DCs), that elicit adaptive immune responses. These cells require the presence of specific amounts and types of cytokines for their differentiation, being affected by the relative abundance of cytokines which decide their functionality.[38] Moreover, the monocytes have a propensity to differentiate into different types of macrophages

and DCs depending on stimuli,[38] due to their inherent plasticity. Since serum or plasma contains many factors, it is likely that the process of differentiation of PBMCs would be affected by these components. The present study aimed to see if the survival of PBMCs is affected by the addition of plasma and the biochemical changes arising due to these effects. Substitution of FCS by plasma would help to better represent *in vivo*-like conditions. Previous reports indicated that plasma and serum treatments promoted immunity, thus indicating an alteration in the metabolic patterns of immune cells. The biochemical changes associated due to the addition of plasma were studied using FTIR spectroscopy, in addition to conventional microscopy, to elucidate plasma-induced changes.

We propose that heat-stable components present in the serum or plasma stimulate the cells, as most cytokines would be degraded during heat inactivation of the plasma/serum. The biochemical component that was altered due to the addition of AHP/NAHP was mainly phospholipids, as identified from its signature absorbance bands in the mid-IR region.[32] Though cell division and proliferation was not affected as evaluated using the method proposed by Mourant et al.,[33] increased survival indicated that AHP/NAHP influenced the metabolic pathways of PBMCs. We show that plasma factors influence the biogenesis of phospholipids (which are essential membrane components) that are required for normal functioning of APCs, as these are involved in processes like endocytosis,[39] autophagy,[40–42] and antigen processing and presentation.[43] Lipids are important components of lipid rafts that are essential for many cellular processes like transport and insertion of membrane proteins that can alter the structure and function of the immune cells and can lead to disease conditions.[44] The analysis of such changes in the membrane components using FTIR has been attempted in this study by monitoring the changes in the higher wavenumber (2852 cm^{-1}), which identified increased signatures of phospholipids in sera-treated samples. Importantly, the addition of NAHP showed similar effects like AHP. These observations have important implications in blood transfusion and treatment of patients with compromised immunity, as factors governing phospholipid metabolism and availability may be considered in addition to other blood parameters for an effective treatment regimen. The present study also examines the implications of such media alterations for routine cell culturing, which would enhance the properties of cells and help in faster monitoring using inexpensive methods like FTIR spectroscopy. On the other hand, the present study also highlights the limitations of results obtained from the current *in vitro* systems and cell growth conditions, which may not accurately reflect prevalent *in vivo* conditions. Interestingly, though a similar survival is obtained using AHP or NAHP instead of FCS, there are differences among the groups which can be identified by exploiting the spectral analysis techniques like PCA on the obtained spectral data. FTIR spectroscopy can thus be used as an inexpensive and rapid method to monitor biochemical changes in cells during routine laboratory practices.

5 Conclusions

Our study highlights the effect of plasma supplementation for human PBMCs under *in vitro* culture conditions. We not only observed a change in biochemical composition by inclusion of AHP/NAHP in the media used for culturing PBMCs, but also observed that such changes affect the survival through membrane biogenesis and differentiation of the adherent PBMCs which are precursors of macrophages and DCs (as observed both by light microscopy and FTIR spectroscopy). The present study highlights how alterations in FTIR spectra may reflect structural changes in addition to biochemical changes. It demonstrates that FTIR spectroscopy may be applied for elucidating cellular mechanisms.

Acknowledgments

We thank Shirley Steinman for help with data collection.

References

1. J. M. del Castillo et al., "Treatment of recurrent corneal erosions using autologous serum," *Cornea* **21**(8), 781–783 (2002).
2. A. C. Poon et al., "Autologous serum eye drops for dry eyes and epithelial defects: clinical and in vitro toxicity studies," *Br. J. Ophthalmol.* **85**(10), 1188–1197 (2001).
3. S. D. Schulze, W. Sekundo, and P. Kroll, "Autologous serum for the treatment of corneal epithelial abrasions in diabetic patients undergoing vitrectomy," *Am. J. Ophthalmol.* **142**(2), 207–211 (2006).
4. M. Rutgers et al., "Cytokine profile of autologous conditioned serum for treatment of osteoarthritis, in vitro effects on cartilage metabolism and intra-articular levels after injection," *Arthritis Res. Ther.* **12**(3), R114 (2010).
5. S. Booth et al., "The impact of acute strenuous exercise on TLR2, TLR4 and HLA.DR expression on human blood monocytes induced by autologous serum," *Eur. J. Appl. Physiol.* **110**(6), 1259–1268 (2010).
6. T. Koga and M. Meydani, "Effect of plasma metabolites of (+)-catechin and quercetin on monocyte adhesion to human aortic endothelial cells," *Am. J. Clin. Nutr.* **73**(5), 941–948 (2001).
7. U. J. Sachs et al., "Mechanism of transfusion-related acute lung injury induced by HLA class II antibodies," *Blood* **117**(2), 669–677 (2011).
8. X. D. Nguyen et al., "Collection of autologous monocytes for dendritic cell vaccination therapy in metastatic melanoma patients," *Transfusion* **42**(4), 428–432 (2002).
9. U. Zelig et al., "Biochemical analysis and quantification of hematopoietic stem cells by infrared spectroscopy," *J. Biomed. Opt.* **15**(3), 037008 (2010).
10. U. Zelig et al., "Diagnosis of cell death by means of infrared spectroscopy," *Biophys. J.* **97**(7), 2107–2114 (2009).
11. F. Colombo et al., "Evidence of distinct tumour-propagating cell populations with different properties in primary human hepatocellular carcinoma," *PLoS One* **6**(6), e21369 (2011).
12. S. Lordan and C. L. Higginbotham, "Effect of serum concentration on the cytotoxicity of clay particles," *Cell Biol. Int.* **36**(1), 57–61 (2012).
13. R. K. Sahu, S. Mordechai, and E. Manor, "Nucleic acids absorbance in mid IR and its effect on diagnostic variates during cell division: a case study with lymphoblastic cells," *Biopolymers* **89**(11), 993–1001 (2008).
14. J. R. Mourant et al., "Polarized angular dependent spectroscopy of epithelial cells and epithelial cell nuclei to determine the size scale of scattering structures," *J. Biomed. Opt.* **7**(3), 378–387 (2002).
15. H. Y. Holman et al., "IR spectroscopic characteristics of cell cycle and cell death probed by synchrotron radiation based Fourier transform IR spectromicroscopy," *Biopolymers* **57**(6), 329–335 (2000).
16. E. Manor, "Human plasma accelerates immortalization of B lymphocytes by Epstein-Barr virus," *Cell Prolif.* **41**(2), 292–298 (2008).
17. E. Manor et al., "Cytogenetic findings in benign and malignant oral tumors—the role of autologous human plasma," *Br. J. Oral Maxillofac. Surg.* **50**(7), 606–610 (2012).
18. F. Camastra and A. Vinciarelli, *Machine Learning for Audio, Image and Video Analysis*, Springer, London (2008).
19. A. Zwielly et al., "Discrimination between drug resistant and non-resistant human melanoma cell lines using FTIR spectroscopy," *Analyst* **134**(2), 294–300 (2009).
20. A. Salman et al., "Detection and identification of cancerous murine fibroblasts, transformed by murine sarcoma virus in culture, using Raman spectroscopy and advanced statistical methods," *Biochim. Biophys. Acta.* **1830**(3), 2720–2727 (2013).

21. A. Travo et al., "Basis of a FTIR spectroscopy methodology for automated evaluation of Akt kinase inhibitor on leukemic cell lines used as model," *Anal. Bioanal. Chem.* **404**(6–7), 1733–1743 (2012).
22. M. Diem, P. Griffith, and J. Chalmers, *Vibrational Spectroscopy for Medical Diagnosis*, Wiley, New York (2008).
23. R. A. Fisher, "The use of multiple measurements in taxonomic problems," *Ann. Eugen.* **7**(2), 179–188 (1936).
24. G. M. James and T. J. Hastie, "Functional linear discriminant analysis for irregularly sampled curves," *J. R. Stat. Soc. Ser. B (Stat. Methodol.)* **63**(3), 533–550 (2001).
25. A. Salman et al., "Identification of fungal phytopathogens using Fourier transform infrared-attenuated total reflection spectroscopy and advanced statistical methods," *J. Biomed. Opt.* **17**(1), 017002 (2012).
26. A. Salman et al., "Utilizing FTIR-ATR spectroscopy for classification and relative spectral similarity evaluation of different Collectotrichum cocodes isolates," *Analyst* **137**(15), 3558–3564 (2012).
27. C. Huberty, *Applied Discriminant Analysis*, Wiley, New York (1994).
28. K. Fukunaga, *Introduction to Statistical Pattern Recognition*, Academic Press, San Diego (1990).
29. M. Otto, *Chemometrics: Statistics and Computer Application in Analytical Chemistry*, WILEY-VCH, Toronto (1999).
30. B. Everitt, *Cluster Analysis*, 2nd ed., Heinman Educational Books, London (1980).
31. B. Flury and H. Riedwyl, *Multivariate Statistics. A Practical Approach*, Chapman and Hall, London (1988).
32. J. L. R. Arrondo and F. M. Goni, "Infrared studies of protein-induced perturbations of lipids in lipoproteins and membranes," *Chem. Phys. Lipids* **96**(1–2), 53–68 (1998).
33. J. R. Mourant et al., "Vibrational spectroscopy of viable, paired tumorigenic and non-tumorigenic cells," *Proc. SPIE.* **4614**, 109–116 (2002).
34. C. Matthäus et al., "Non-invasive imaging of intracellular lipid metabolism in macrophages by Raman microscopy in combination with stable isotopic labeling," *Anal. Chem.* **84**(20), 8549–8556 (2012).
35. S. E. Holton, M. J. Walsh, and R. Bhargava, "Subcellular localization of early biochemical transformations in cancer-activated fibroblasts using infrared spectroscopic imaging," *Analyst* **136**(14), 2953–2958 (2011).
36. K. J. Chalut et al., "Light scattering measurements of subcellular structure provide noninvasive early detection of chemotherapy-induced apoptosis," *Cancer Res.* **69**(3), 1199–1204 (2009).
37. M. Sankaranarayanapillai et al., "Metabolic shifts induced by fatty acid synthase inhibitor orlistat in non-small cell lung carcinoma cells provide novel pharmacodynamic biomarkers for positron emission tomography and magnetic resonance spectroscopy," *Mol. Imaging Biol.* **15**(2), 136–147 (2013).
38. A. Sica and A. Mantovani, "Macrophage plasticity and polarization: in vivo veritas," *J Clin. Invest.* **122**(3), 787–795 (2012).
39. C. Rauch and E. Farge, "Endocytosis switch controlled by transmembrane osmotic pressure and phospholipid number asymmetry," *Biophys. J.* **78**(6), 3036–3047 (2000).
40. P. Lajoie et al., "The lipid composition of autophagic vacuoles regulates expression of multilamellar bodies," *J. Cell Sci.* **118**(9), 1991–2003 (2005).
41. J. P. Girardi, L. Pereira, and M. Bakovic, "De novo synthesis of phospholipids is coupled with autophagosome formation," *Med. Hypotheses* **77**(6), 1083–1087 (2011).
42. R. W. Roof, I. F. Luescher, and E. R. Unanue, "Phospholipids enhance the binding of peptides to class II major histocompatibility molecules," *PNAS* **87**(5), 1735–1739 (1990).
43. S. Krishnan et al., "Alterations in lipid raft composition and dynamics contribute to abnormal T cell responses in systemic lupus erythematosus," *J. Immunol.* **172**(12), 7821–7831 (2004).
44. V. Michel and M. Bakovic, "Lipid rafts in health and disease," *Biol. Cell.* **99**(3), 129–140 (2007).